SUPPLEMENTARY INFORMATION
Supplementary Materials and Methods

Cell lines and culture

Human PCa cell line (PC-3) and mouse PCa cell line (RM-1) were purchased from the Shanghai Chinese Academy of Sciences cell bank (Shanghai, China). All cell lines were cultured in Roswell Park Memorial Institute (RPMI)-1640 medium (Life Technologies, Carlsbad, CA, USA) supplemented with 1% penicillin-streptomycin and 10% fetal bovine serum (FBS; Life Technologies). 5% CO_2 and 37 °C were maintained throughout the incubation.

Patients and tissue samples

A total of 222 paraffin-embedded PCa tissues, including 192 primary PCa tissues (132 without BM and 60 with BM) and 30 paired samples of metastatic bone tissues, were obtained during surgery or needle biopsy at The First Affiliated Hospital of Sun Yat-sen University (Guangzhou, China) between January 2012 and March 2020. The approval number was [2014]A-011. Tissue samples underwent pathologist review for verification. Clinicopathological data of the 185 consecutive PCa patients (7/192 lost to follow-up), including age, differentiation, serum PSA, Gleason grade, and Bone metastasis (BM) status, were obtained. The use of these specimens and the patients' clinical information was approved by the Institutional Research Ethics Committee. The median BHLHE22 expression in PCa tissues was used to stratify the high and low expression of BHLHE22.

Plasmids and transfection

Transient transfection and lentivirus production were performed using Lipofectamine 3000 reagent (Invitrogen, Waltham, MA, USA). The transfection efficiency was verified by qRT-PCR and western blotting. For lentivirus production, a lentiviral expression plasmid and third-generation lentivirus packaging vectors (pLP1, pLP2, pLP/VSVG) (ViraPower Packaging Mix, Thermo Fisher Scientific, Waltham, MA, USA) were used to transfect HEK293FT cells. At 48–72 h post-transfection, lentiviruses were collected to infect PCa cell lines. Drug-resistant clones (Puromycin, G418) were then selected to generate a stable cell line. The human *BHLHE22* cDNA (NM_152414.5) was cloned into a pCDH plasmid expression vector (pCDH-FLAG- BHLHE22-Puro). pCDH-Puro vector was used as a control. Mouse *Bhlhe22* cDNA (NM_021560.4) was cloned into a pLVX plasmid expression vector (pLVX-FLAG-Bhlhe22-Hyg). The pLVX-Hyg vector was used as a control. The *Prmt5* cDNA (NM_013768.3) was cloned into a pLVX plasmid expression vector (pLVX-HA-Prmt5-Puro). The pLVX-Puro vector was used as a control. Two short hairpin RNAs (shRNAs) against *Prmt5* (targeting sequences: shRNA Prmt5#1, 5′-GGTGAACACAGTGCTTCATGG-3′; shRNA Prmt5#, 5′-CCATGAAGCACTGTGTTCACC-3′) were cloned into the pLKO.1-puro lentivirus vector (#8453, Addgene, Watertown, MA, USA).

Western blotting

Western blotting was carried out as previously described [1]. Target proteins were detected using the following primary antibodies: anti-BHLHE22 (Invitrogen; PA5-64189,1:500), anti-PRMT5 (Invitrogen; MA5-32160, 1:1,000), anti-CSF2 (Proteintech, Rosemont, IL, USA; 17762-1-AP, 1:1,000), anti-Flag (Cell Signaling Technology, Danvers, MA, USA; 14793, 1:1,000), anti-HA (Cell Signaling Technology;

3724, 1:1,000), anti-H4R3me2a (Invitrogen; PA5-102612, 1:500), anti-H4R3me2s (ActiveMotif, Carlsbad, CA, USA; 61187, 1:500), anti-H3R2me2a (Epigentek, Farmingdale, NY, USA; A-3714, 1:500), anti-H3R2me2s (Epigentek; A-3705, 1:500), anti-H3R8me2a (ActiveMotif; 39651, 1:500), anti-H3R8me2s (Epigentek; A-3706, 1:500). Anti-GAPDH (Proteintech; 60004-1, 1:20,000) and anti-H3 (Proteintech; 17168-1, 1:2,000) antibodies were used as loading controls.

Quantitative real-time reverse transcription PCR

Total RNA was extracted using TRIzol and reverse-transcribed to cDNA using TaqMan reverse transcription reagents. Quantitative real-time PCR was then conducted using the cDNA as the template and SYBR Green master mix on a ViiA7 real-time PCR system (Applied Biosystems, Foster City, CA, USA). GAPDH or histone H3 were used as loading controls. Relative fold expressions were calculated using the comparative threshold cycle ($2^{-\Delta\Delta Ct}$) method [2]. Primers are listed in online supplemental table S4.

IHC

Immunohistochemistry assays were performed following our previously described method [1]. Formalin-fixed paraffin embedded (FFPE) tumor tissues were cut in 4 μm sections. Slides were then incubated with BHLHE22 (Invitrogen; PA5-64189, 1:2,500), PRMT5 (Invitrogen; MA5-32160, 1:200), CSF2 (Proteintech; 17762-1-AP, 1:200), CD4 (Cell Signaling Technology; 25229 and 93518, 1:200), CD8 (Cell Signaling Technology; 98941 and 85336, 1:200), CD33 (Invitrogen; PA5-120758, 1:200), Gr-1 (Invitrogen; 14-5931-82, 1:100), S100A9 (Cell Signaling Technology; 73425, 1:800), Ki-67 (Abcam, Cambridge, MA, USA; ab16667, 1:200), CHGA (Proteintech; 60135-2-Ig; 1:2000), SYP (Proteintech; 67864-1-Ig; 1:1000), NSE (Proteintech; 66150-1-Ig; 1:2500), and AR (Cell Signaling Technology; 5153S; 1:500) antibodies at 4 °C overnight.

Two independent pathologists selected ten randomly selected fields of view. The IHC-score was recorded based on the mean value of the selected fields, which was calculated as staining intensity score × proportion of positive tumor cells score. The staining intensity was scored as: 0 (no staining), 1 (light yellow), 2 (yellow brown), and 3 (brown). The proportion of positive tumor cells was scored as: 0 (no positive tumor cells), 1 (<10% positive tumor cells), 2 (10–35% positive tumor cells), 3 (36–70% positive tumor cells), and 4 (>70% positive tumor cells). Based on the IHC-score, we defined target gene expression as: negative staining (0 score), weak staining (1–4 score), moderate staining (5–8 score), and strong staining (9–12 score). The median IHC scores of the target genes were used as the cutoff values to stratify high and low expression.

IF

Immunofluorescence assays were performed following our previously described method [1]. For cellular IF staining, cells were seeded in 24-well plates and cultured on coverslips. The coverslips were then incubated with BHLHE22 (Invitrogen; PA5-64189, 1:100) and PRMT5 (Invitrogen; MA5-32160, 1:50) antibodies. Alexa Fluor 488 and 594 goat anti-rabbit were used as secondary antibodies (Cell Signaling Technology). For tissue IF staining, tumor tissue slides were incubated with BHLHE22 (Invitrogen; PA5-64189, 1:100), CSF2 (Proteintech; 17762-1-AP, 1:100), CD4 (Cell Signaling Technology; 25229, 1:100), CD8 (Cell Signaling Technology; 98941 and 85336, 1:100), CD33 (Invitrogen; PA5-120758,

1:100), Gr-1 (Novus, St. Louis, MO, USA; NBP3-11978, 1:100). Then, the slides were stained with the PANO Reagents PPD480, PPD520, PDD570, and PPD650 using a PANO 5-plex IHC Kit (#10203100050, # 10144100050, Panovue, Guangzhou, China) according to the manufacturer's instructions. Nuclei were counterstained using DAPI (Sigma-Aldrich, St. Louis, MO, US). The fluorescent signals were detected using a Zeiss LSM710 confocal microscope (Carl Zeiss, Oberkochen, Germany). The images were analyzed using Image J 1.52V.

Migration, invasion assay

Migration, invasion, and wound healing assays were performed following our previous described methods [3]. Migration & invasion assays were performed using a Transwell chamber (#3422, Corning Inc., Corning, NY, USA) with or without Matrigel (#356234, BD Biosciences, San Jose, CA, USA) coating. At 24–48 h later, the cells that had invaded/migrated into the lower chamber were counted under a microscope (200×).

Cell proliferation assay

Cell viability was determined by colony formation assay following our previous described methods[3]. Cell cycle was measured using flow cytometry. Detailed information about the cell cycle analysis is described in our previous study[3].

Histology, TRAP staining

Femurs and tibiae were fixed overnight in paraformaldehyde solution (4%) followed by decalcification in 4.3% EDTA for 1 week, then embedded in paraffin wax. Sections were used by H&E stained, or stained with a TRAP kit (387A-1KT; Sigma-Aldrich) according to the manufacturer's protocol. $TRAP^+$-osteoclasts were counted on a 3 mm length of endocortical surface and observed on an optical microscope (Olympus, Tokyo, Japan).

T cells and $CD11b^+Gr\text{-}1^+$ cells isolation

T cells and $CD11b^+Gr\text{-}1^+$ myeloid cells were isolated from the spleens of tumor-bearing mice using a Mouse $CD8^+$ T Cell Isolation Kit (#19853, Stemcell Technologies, Vancouver, Canada) and a Mouse $CD11b^+Gr1^+$ cells Isolation Kit (#19867, Stemcell Technologies). Cell purity was checked by flow cytometry analysis using anti-CD3/CD8 (T cells, >90%) and anti-CD11b/Gr-1 antibodies ($CD11b^+Gr\text{-}1^+$ cells, >95%). Trypan blue dye exclusion was used to check cell viability. The isolated cells were cultured in complete RPMI medium supplemented with 10% FBS at 5% CO_2, 37 °C, and used for further *in vitro* co-culture assays.

T cell suppression assay

Twenty-four well plates were coated with anti-CD3 (1 μg/ml) and anti-CD28 (1 μg/ml) in phosphate-buffered saline (PBS) for 2 h (with noncoated wells as controls). Isolated $CD8^+$ T cells were labeled with CFSE (2 μM) and then incubated with $CD11b^+Gr\text{-}1^+$ cells in 24-well plates (at T

cells/CD11b$^+$Gr-1$^+$ cells ratios of 1:0, 1:1, and 1:5). The plates were placed into the incubator. T cell proliferation was measured by flow cytometry analysis of CFSE peaks after 4 d of coculture.

RM-1 and CD11b$^+$Gr-1$^+$ cells co-culture assay

RM-1 cells (RM-1-Vector, RM-1-Bhlhe22, RM-1-Bhlhe22-shNC, and RM-1-Bhlhe22-Prmt5-sh) were seeded in 6-well plates at a density of 1×10^6 cells/well. Isolated CD11b$^+$Gr-1$^+$ cells were labeled with CFSE (2 μM) and then incubated with RM-1 cells in 24-well plates (at an CD11b$^+$Gr-1$^+$/RM-1 cell ratio of 1:1). CD11b$^+$Gr-1$^+$ cells expansion *in vitro* was measured by flow cytometry of CFSE peaks after 5 d of coculture. In CSF2 blocking experiments, the co-culture system was blocked using anti-CSF2 antibody (20 ng/ml, BioXcell, New Haven, CT, USA). Recombinant murine CSF2 (20 ng/ml, PeproTech, Rocky Hill, NJ, USAS) was used as a positive control. Non-treated and non-co-cultured CD11b$^+$Gr-1$^+$ cells were used as the vehicle group. In the Prmt5 inhibition experiments, the co-culture group of RM-1-Bhlhe22 was treated with GSK591 (5 μM, TargetMol, Boston, MA, USA), and isotype IgGs were used as controls.

CD11b$^+$Gr-1$^+$ cells depletion in vivo

The efficacy of CD11b$^+$Gr-1$^+$ cells depletion was evaluated in RM-1-Bhlhe22 cells. C57BL/6J mice were left cardiac ventricle (LCV)-injected with RM-1-Bhlhe22 and randomly divided into anti-Gr-1 (200 μg per mouse twice a week, intraperitoneal injection, BioXcell) and isotype IgGs groups. At 30 d post-injection, BM bone marrow samples were harvested for further study.

Bone metastatic mouse models

All mouse experimental procedures were approved by The Institutional Animal Care and Use Committee of Sun Yat-sen University (approval-No. SYSU-IACUC-2022-000178). For the bone metastases study, BALB/c nude and C57BL/6J mice (male, 4–6 weeks old) were anesthetized and 2×10^5 PCa cells (PC-3 or RM-1) in 100 μl PBS were inoculated into the left cardiac ventricle. C57BL/6J mice were shaved before imaging. Bone metastases were monitored twice a week using bioluminescent imaging (IVIS, Caliper Life Sciences, Hopkinton, MA, USA). Osteolytic bone lesions and trabecular sections were analyzed using Micro-CT scanning (SIEMENS, Munich, Germany).

Micro-CT analysis

Fixed hind limbs were scanned on a micro-CT scanner (SIEMENS, Munich, Germany). The 3D models were reconstructed by NRecon. After digitally eliminating cortical bone, trabecular volume of interest was determined starting from the metaphysis and included all trabeculae in a 1 mm3 region. Bone parameters were analyzed using CTAn and CTVol.

Mouse treatments

For the mouse CD11b$^+$Gr-1$^+$ cells infiltration *in vivo* assay: at 3 d post LCV-injection with RM-1-Vector or RM-1-Bhlhe22, C57BL/6J mice were treated with anti-CSF2 antibody (20 μg per mouse twice a week, intraperitoneal injection, BioXcell), and isotype IgGs were used as the control. Non-tumor-bearing mice were treated with recombinant murine CSF2 (0.6 μg per mouse twice a week, subcutaneous injection,

PeproTech), and isotype IgGs were used as the control. At 3 d post LCV-injection with RM-1 cells (RM-1-Vector, RM-1-Bhlhe22, and RM-1-Bhlhe22-Prmt5-sh), the RM-1-Bhlhe22 group were treated with GSK3326595 (50 mg/kg/day, oral, TargetMol), and isotype IgGs were used as the control.

For CSF2 neutralization and ICT combination therapies: At 3 d post LCV-injection with RM-1-Bhlhe22, C57BL/6J mice were treated with anti-CSF2 antibody alone (20 μg per mouse twice a week, intraperitoneal injection, BioXcell) or anti-PD-1 alone (200 μg per mouse twice a week, intraperitoneal injection, BioXcell) or combined anti-CSF2 with anti-PD-1 (as above), and isotype IgGs were used as the control.

For the PRMT5 inhibitor and ICT combination therapies: At 3 d post LCV-injection with RM-1-Bhlhe22, C57BL/6J mice were treated with GSK3326595 alone (50 mg/kg/day, oral, TargetMol) or anti-PD-1 alone (200 μg per mouse twice a week, intraperitoneal injection, BioXcell) or combined GSK3326595 with anti-PD-1 (as above), and isotype IgGs were used as the control.

For the osteoclasts inhibition: At 3 d post LCV-injection with RM-1-Vector and RM-1-Bhlhe22, C57BL/6J mice were treated with Zoledronic acid (120 μg/kg twice a week, subcutaneously, TargetMol)[4, 5] and isotype IgGs were used as the control.

Flow cytometry

BM bone marrow samples were harvested from experimental mice and cut into small fragments after removal of the soft tissue. Bone marrow cells were released by gentle grinding. Then, the BM bone marrow samples were digested using a mixture of 1.25 mg/mL collagenase D (#11088866001, Roche, Basle, Switzerland), 0.85 mg/ml collagenase V (#C9263, Sigma), 50 μg/ml DNase I (#DN25, Sigma), and 1 mg/ml Dispase II (#D4693, Sigma) for 40 min (37 °C, 80 rpm). Erythrocytes were removed using a red blood cell lysis buffer (Sigma). After centrifugation and resuspension, single cells were added to 5 ml flow cytometry tubes and blocked with anti-CD16/CD32 antibodies (#101302, Biolegend, San Diego, CA, USA) before being stained for flow cytometry. Mouse tumor-infiltrating viable immune cell ($CD45^+$ and $7AAD^-$), $CD4^+$ T cells ($CD3^+$ and $CD4^+$), $CD8^+$ T cells ($CD3^+$ and $CD8^+$), immunosuppressive neutrophils and monocytes ($CD11b^+$ and $Gr\text{-}1^+$), monocytes ($CD11b^+$, $Gr\text{-}1^+$, $Ly6C^{hi}$, and $Ly6G^-$), neutrophils ($CD11b^+$, $Gr\text{-}1^+$, $Ly6C^{lo}$, and $Ly6G^+$), NK cells ($CD3^-$ and $NK1.1^+$), Tregs ($CD4^+$, $CD25^+$, and $Foxp3^+$), γ/δ T cells (TCR γ/δ^+),macrophages ($CD11b^+$ and $F4/80^+$), M1 macrophages ($CD11b^+$, $F4/80^+$, and $CD86^+$), M2 macrophages ($CD11b^+$, $F4/80^+$, and $CD206^+$), $CD8^+$ T cell phenotype ($IFN\text{-}\gamma^+$ and $PD\text{-}1^+$), $Arg\text{-}1^+Gr\text{-}1^+$ cells and cell proliferation marker (Ki-67) were analyzed.

Intracellular cytokine staining was performed by fixing and permeabilizing extracellularly stained cells according to the manufacturer's instructions using the Fixation/Permeabilization Solution Kit (Thermo Fisher Scientific Life Sciences). For intracellular IFN-γ staining, cells were stimulated with PMA (5 ng/ml) and ionomycin (500 ng/ml; Sigma-Aldrich) for 4 h. After the staining procedure, samples were run on a CytoFLEX S Flow Cytometer (Beckman, Indianapolis, IN, USA) and the data were analyzed using FlowJo V10.6.2 (Flowjo, LLC, Ashland, OR, USA). The staining antibodies used are listed in online supplemental table S5.

Cytokine array

The Cytokine Array was examined according to the manufacturer's instructions (#AAM-CYT-2, Raybiotech, Peachtree Corners, GA, USA). RM-1-Bhlhe22 and RM-1-Vector cells were cultured in a low

concentration serum medium for 48 h, then supernatants were collected. Cytokine Array membranes were blocked at room temperature for 1 h. 700 µl of supernatants were added to the membranes and incubated at 4 °C overnight. After washing twice, the membranes were incubated with 2 ml of streptavidin-horseradish peroxidase (HRP) at room temperature for 2 h. Then, 0.5 mL of detection mixture solution was added to each membrane, and digital images were collected using a camera system (ImageQuant LAS4000, GE Healthcare, Chicago, IL, USA). The cytokines detected are listed in online supplemental table S6.

RNA-seq

An RNA Extraction Kit (#TR205-200, Tianmo, Beijing, China) was used to extract RNA from *BHLHE22* overexpression cell lines, including PC-3-BHLHE22 and RM-1-Bhlhe22. Each group had three samples and vector cells were used as control. The RNA quality was evaluated using an Agilent Bioanalyzer 2100 (Agilent technologies, Santa Clara, CA, US). The RNA concentration and purity were measured using a Qubit®3.0 Fluorometer (Life Technologies) and a Nanodrop One spectrophotometer (Thermo Fisher Scientific). Sinotech Genomics Corporation (Shanghai, China) performed the library construction and sequencing. The libraries were examined using the Agilent2100 (Agilent) and sequenced on the Illumina NovaSeq 6000 platform using the paired-end option (Illumina, San Diego, CA, USA).

DNA pulldown assay

Based on the site sequences predicted by the JASPAR database, we designed four 50–150 bp 5'-biotin labeled DNA probes (Focobio, Guangzhou, China). DNA pulldown was performed according to the manufacturer's instructions (#R5125, Focobio). Briefly, cells were lysed in ice-cold lysis buffer (Tris-HCl, EDTA, and 1% Triton X-100) in addition of phenylmethylsulfonyl fluoride (PMSF) and a protease inhibitor cocktail (Cell Signaling Technology). The biotin-labeled DNA probes were coupled with streptavidin magnetic beads, and then incubated with cell lysates at room temperature for 2 h. Non-coupled streptavidin magnetic beads were used as the control. After incubation, the mixture was eluted using an elution buffer. The beads were precipitated in a magnetic rack and eluents were collected for further study.

Co-IP assay

HEK293T cells were transfected with Flag-Bhlhe22 (NM_021560.4) or HA-Prmt5 (NM_013768.3) expressing plasmids. Co-IP assays were performed using HEK293T, RM-1-Vector, and RM-1-Bhlhe22 cell lines. Cells were lysed in ice-cold lysis buffer (Tris-HCl, EDTA, and 1% Triton X-100) with the addition of PMSF and a protease inhibitor cocktail (Cell Signaling Technology). Lysates were then incubated with anti-BHLHE22 (#PA5-64189, Invitrogen), or anti-PRMT5 (#MA5-32160, Invitrogen) antibodies, and protein G-conjugated agarose, or Flag, HA affinity agarose (Sigma-Aldrich), at 4 °C overnight. After washing six times, the mixture was eluted using an elution buffer. The beads were precipitated via high-speed centrifugation (8,000g, 5min), and eluents were collected for further study.

Silver stain

The eluents of the DNA pulldown and Co-IP assays were examined using SDS-PAGE. Then, the gels were stained with a Pierce™ Silver Stain Kit (#24612, Thermo Scientific) according to the

manufacturer's instructions. For protein identification, all differentially expressed bands were excised and analyzed using mass spectrometry.

Mass spectrometry

Liquid chromatography/tandem mass spectrometry (LC-MS/MS) was used to identify the co-factors of Bhlhe22. The differentially expressed bands were collected as described above. The bands were enzymatically dissociated to generate peptides. The peptides from the nanoViper C18 column were analyzed using the Q-Exactive system (ThermoFisher Scientific) equipped with a nano-flex ion source. The mass resolution for a full MS scan was set to 70, 000 (at m/z 400). The mass range window was set to 350–2,000 m/z for MS scanning and the maximum ion fill time (IT) was 50 ms. All peptides identified were checked by manual interpretation of the spectra.

Luciferase reporter assay

The pGL4.10-Csf2-promoter and Renilla luciferase vector were cotransfected into PCa cell lines. The pGL4.10-Csf2-promoter, pLVX-Bhlhe22, and Renilla luciferase vectors were cotransfected into HEK293T cell lines. After 48 h, luciferase activities were detected using a Dual-Luciferase Reporter Assay kit (Promega, Madison, WI, USA) according to the manufacturer's instructions. The *Csf2* promoter constructs, including *Csf2*-promoter-FL, *Csf2*-promoter-P1-Wt, and *Csf2*-promoter-P1-Mut, were generated by amplification of a genomic DNA sequence by PCR and then inserted into the pGL4.10-basic plasmid (#46387, Addgene).

ChIP assay

The ChIP assay was performed using the SimpleChIP Plus Enzymatic Chromatin IP Kit (Cell Signaling Technology) according to the manufacturer's instructions. Briefly, indicated cells were fixed with 1% formaldehyde to cross-link the proteins to DNA. Sonication was used to shear the DNA into small fragments. Chromatin supernatants were immunoprecipitated overnight at 4 °C using anti-BHLHE22 (Invitrogen; PA5-64189,1:50), anti-PRMT5 (Invitrogen; MA1-25470, 1:100), anti-H4R3me2a (Invitrogen; PA5-102612, 1:50), anti-H4R3me2s (ActiveMotif; 61187, 1:50), anti-H3R2me2a (Epigentek; A-3714, 1:50), anti-H3R2me2s (Epigentek; A-3705, 1:50), anti-H3R8me2a (ActiveMotif; 39651, 1:50), anti-H3R8me2s (Epigentek; A-3706, 1:50) and anti-IgG antibodies using protein G magnetic beads. Then, the cross-linked DNA-Protein complexes were eluted and the crosslinks were reversed. DNA was purified on a column and analyzed using PCR. All ChIP primers are listed in online supplemental table S7.

Bioinformatic analyses

The genomic and clinical profiles of patients in the TCGA-PRAD dataset were analyzed in cBioPortal [6, 7]. BM had occurred in 10 patients, and 80 patients had no BM (overall survival (OS) ≥ 5 years). The GSE77930 expression profile (URL: https://www.ncbi.nlm.nih.gov/geo/query/acc.cgi?acc=GSE77930) was downloaded from GEO (https://www.ncbi.nlm.nih.gov/geo/). Differentially expressed genes between the BHLHE22 overexpression group and the Vector group were analyzed using the limma package in the R software with a P value threshold of 0.05 and a 1.5-fold change. Based on the TCGA

dataset and our RNA-seq data, differentially expressed genes were subjected to Gene Set Enrichment Analysis (GSEA) (https://www.gsea-msigdb.org/gsea/index.jsp) and Gene Ontology (GO) enrichment analysis (https://david.ncifcrf.gov). The median of *BHLHE22* expression was used as the cutoff. For Kaplan–Meier analysis, the cutoff value was selected based on ROC Curve analysis.

Statistical analyses

Student's t tests were performed to identify differentially expressed genes in the RNA-seq analyses of PC-3 and RM-1 cells ($P < 0.05$, fold change > 1.5). Statistical analyses were performed using GraphPad Prism 9.0 (GraphPad Inc., La Jolla, CA, USA) and SPSS 19.0 (IBM Corp., Armonk, NY, USA). Data are presented as the mean ± standard deviation (SD). The quantitative experiments were conducted independently at least three times. Quantitative data were analyzed using either one-way analysis of variance (ANOVA) (multiple groups) or t tests (normally distributed data, two groups)/Mann–Whitney U test (non-normally distributed data, two groups). Categorical variables and constituent ratios were compared using the $\chi 2$ test. Survival analysis was estimated using Kaplan–Meier curves and log-rank tests. The correlation between the two parameters was determined using Spearman rank correlation analysis. $P < 0.05$ (two-tailed) was considered statistically significant. All statistically significant values shown in figures are indicated as follows: ns, not significant, *$P < 0.05$, **$P < 0.01$, ***$P < 0.001$.

Supplementary Table 1

Clinicopathological features of 185 patients with PCa

Parameters	Number of cases (n = 185)	BHLHE22 expression Low (n = 93)	High (n = 92)	P-value (χ^2 test)
Age (years)				
< 73	92	50	42	
≥ 73	93	43	50	0.27
Differentiation				
Well/moderate	86	49	37	
Poor	99	44	55	< 0.01**
Serum PSA				
< 75.6	92	55	37	
≥ 75.6	93	38	55	< 0.05*
Gleason grade				
≤ 7	78	49	29	
> 7	107	44	63	< 0.01**
BM status				
nBM	125	73	52	
BM	60	20	40	< 0.01**
AR Score				
(-)	15	5	10	
(+)	59	21	38	
(++)	46	25	21	
(+++)	65	42	23	< 0.01**
NE marker				
CHGA (-)	165	89	76	
CHGA (+)	20	4	16	< 0.01**
NSE (-)	173	90	83	
NSE (+)	12	3	9	0.07
SYP (-)	168	89	79	
SYP (+)	17	4	13	< 0.05*

Abbreviation: PSA, Prostate-specific Antigen; BM, Bone Metastasis; nBM, Non-bone Metastasis; AR, Androgen Receptor; NE, Neuroendocrine; CHGA, Chromogranin A; NSE, Neuron Specific Enolase; SYP, Synaptophysin.

Supplementary Table 2

Sequence of DNA pulldown probes

Probes	Sequence
P1	5′-GCCAGGAAATC**CAAATATGCC**TGGAGGCCCCTCAAAAAGGAGAG GCTAGCCAGAGGCTGATGTGGCTGCAGAATTTACTTTTCCTGGGCATTG TGGT-3′
P2	5′-AACACCACCAGCATACACACATGACTGAAGAGATA**CACATATGTA** TCCCCATGGTCTCAAACTTCCTGTATAGGAAGGCTTGGG-3′
P3	5′-GGCACCTGTAG**ACCATATCCT**TGACGTGAGTCTTGACTCTGGGGC CTCTGCTTTCCTCTTAGCCACCACCCT**GCCACACGCT**TGGGCTAAGAC GAATGCCTTTAGTTCTTCA-3′
P4	5′-GTGTTGACTTCCTCTTGTGATAAAGATCCTGGGGCA**GCCACACGCT** TCTGGTTCCCCCAGGGCCCATGTCAAGGGACACTCCCCGGAAACTCCTTC CAGAGGGTTCTCTCCTGGCCTTGTGGGCTGGGAGGCCAAAGAGGGGTCA CTCCA**CCCATCTGGT**-3′

Bolded letters indicate the predicted binding sequence in the promoter of *Csf2*.

Supplementary Table 3

Sequence of P1-WT and P1-Mut

P1	Sequence
WT	5′-GCCAGGAAATC**CAAATATGCC**TGGAGGCCCCTCAAAAAGGAGAG GCTAGCCAGAGGCTGATGTGGCTGCAGAATTTACTTTTCCTGGGCATTG TGGT-3′
Mut	5′-GCCAGGAAATC**TTTTTTTTTT**TGGAGGCCCCTCAAAAAGGAGAG GCTAGCCAGAGGCTGATGTGGCTGCAGAATTTACTTTTCCTGGGCATTG TGGT-3′

Bolded letters indicate the wild-type (WT) or mutated (Mut) binding sequence in the promoter of *Csf2*.

Supplementary Table 4

List of primers used for qRT-PCR

Real-time PCR primer (Human)	Sequence
BHLHE22- Forward	5′-CTGCGGCTTAACATCAATGCCC-3′
BHLHE22- Reverse	5′-GTGGCGATCTTGGAGAGCTTTC-3′
PRMT5- Forward	5′-CTAGACCGAGTACCAGAAGAGG-3′
PRMT5- Reverse	5′-CAGCATACAGCTTTATCCGCCG-3′
CSF2- Forward	5′-GGAGCATGTGAATGCCATCCAG-3′
CSF2- Reverse	5′-CTGGAGGTCAAACATTTCTGAGAT-3′
GAPDH- Forward	5′-GTCTCCTCTGACTTCAACAGCG-3′
GAPDH- Reverse	5′-ACCACCCTGTTGCTGTAGCCAA-3′

Real-time PCR primer (Mouse)	Sequence
Bhlhe22- Forward	5′-GAAGCTCTCCAAAATCGCCACG-3′
Bhlhe22- Reverse	5′-CCTTGGTTGAGGTAGGCGACTA-3′
Prmt5- Forward	5′-CCTGCTTTACCTTCAGCCATCC-3′
Prmt5- Reverse	5′-GCACAGTCTCAAAGTAGCCTGC-3′
Csf2- Forward	5′-AACCTCCTGGATGACATGCCTG-3′
Csf2- Reverse	5’-AAATTGCCCCGTAGACCCTGCT-3′
GAPDH- Forward	5′-CATCACTGCCACCCAGAAGACTG-3′
GAPDH- Reverse	5′-ATGCCAGTGAGCTTCCCGTTCAG-3′

Supplementary Table 5

List of reagents used for flow cytometry

Marker	Dye	Brand
CD45	FITC, BV605, Alexa Fluro700	Biolegend
7AAD	PC5.5	BD Pharmingen
CD11b	PE, PC7	Biolegend
Gr-1	PE, APC-Cy7	Biolegend
Ly6G	APC	Biolegend
Ly6C	BV421	Biolegend
Agr-1	PE, Alexa Fluro 700	Biolegend, ThermoFisher
CD3	BV650, Alexa Fluro700	Biolegend
CD4	BV421, BV605	Biolegend
CD8	BV510	Biolegend
PD-1	PE, APC	Biolegend
IFN-γ	APC	Biolegend
CD25	APC-Cy7	Biolegend
Foxp3	FITC	Biolegend
F4/80	FITC	Biolegend
CD86	PC7	Biolegend
CD206	APC	Biolegend
NK1.1	BV650	Biolegend
Ki-67	PE	Biolegend
TCR γ/δ	FITC, APC	Biolegend

Supplementary Table 6

List of cytokines in the cytokine array

Pos	Pos	Neg	Neg	Ccl21	Ccl27	Ccl11	Csf3	Csf2	Il-2	Il-3	Il-4
Pos	Pos	Neg	Neg	Ccl21	Ccl27	Ccl11	Csf3	Csf2	Il-2	Il-3	Il-4
Il-5	Il-6	Il-9	Il-10	Il12-p40/p70	Il12-p70	Il-13	Il-17	Ifn-γ	Cxcl1	Leptin	Ccl2
Il-5	Il-6	Il-9	Il-10	Il12-p40/p70	Il12-p70	Il-13	Il-17	Ifn-γ	Cxcl1	Leptin	Ccl2
Ccl12	Ccl3	Cxcl2	Ccl19	Ccl5	Scf	Tnfrsf1a	Ccl17	Timp-1	Tnf-α	Tpo	Vegf
Ccl12	Ccl3	Cxcl2	Ccl19	Ccl5	Scf	Tnfrsf1a	Ccl17	Timp-1	Tnf-α	Tpo	Vegf
											Pos
											Pos

Supplementary Table 7

List of primers used for ChIP-qPCR

CSF2 ChIP-qPCR primer (Human)	Sequence
Primer1- Forward	5′-CCACTCAGTATCTCCCAAAC-3′
Primer1- Reverse	5′-GGCTGTAGACCACAATGC-3′
Primer2- Forward	5′-AAGTGTGGCTCATGTTAGAT-3′
Primer2- Reverse	5′-TGTATGCTGGTGGTGTTG-3′
Primer3- Forward	5′- GGCACCTGTAGACCATATC-3′
Primer3- Reverse	5′- GTGGAACTCAGGACAAGAC-3′
Primer4- Forward	5′-GTGTTGACTTCCTCTTGTGA-3′
Primer4- Reverse	5′-ACCAGATGGGTGGAGTGA-3′

Csf2 ChIP-qPCR primer (Mouse)	Sequence
Primer1-F	5′-GGCTGTCGGTTCTTGGAA

orward Primer 1 - Reverse Primer 2 - Forward Primer	-3′ 5′-CTACACTGACTTGACCTTGTGATTCTC-3′ 5′-AGTGTAGTCCGACTTCACTTCAGTGTC-3′ 5′-GTCTGACTCTTGTGCTCTGTC-3′

er2-Reverse Primer3-Forward Primer3-Reverse	AGAATG-3′ 5′-CATCTATTGAGTCCTTCTTACCT-3′ 5′-CACTATCTATGGCTCCCTTC-3′ 5′-GATGAGGACATGGATACTACA-3′

ePrimer4-ForwardPrimer4-Reverse

Supplementary Figure 1

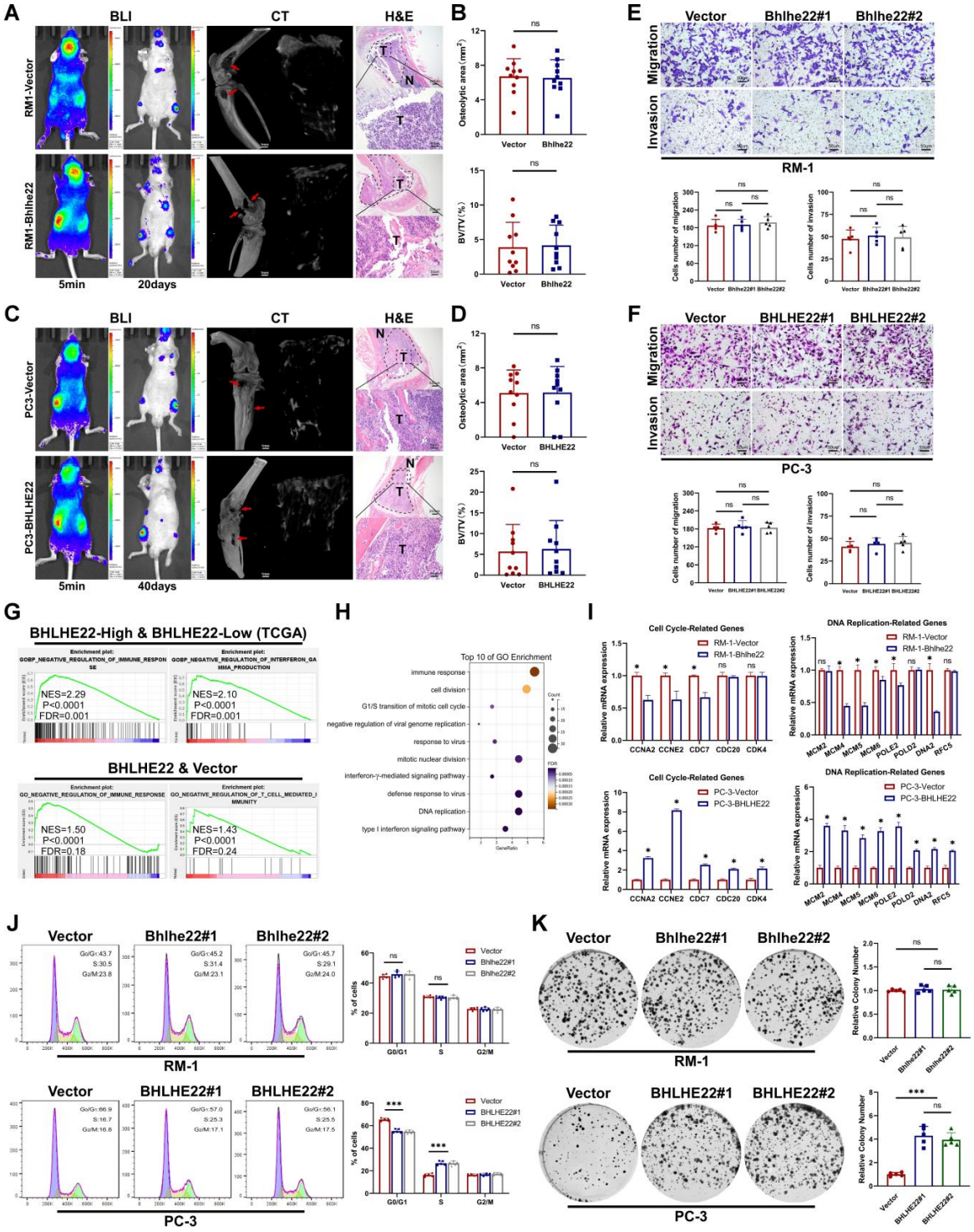

Supplementary Figure 1. BHLHE22 promotes bone metastasis in an immunity-associated manner. (**A** and **C**) Representative BLI signal, micro-CT (arrows indicate osteolytic lesions. Bars, 1mm) and H&E (T, tumor; N, the adjacent nontumor tissues. Bars, 200 μm and 50 μm) images of BALB/c nude mice LCV-injected with RM-1 (A) and PC-3 (C) cells. (**B** and **D**) Quantification of osteolytic areas and bone parameters in the indicated cells. BV/TV, bone/tissue volume ratio. ns, not significant; t test. (**E** and **F**) Representative images and quantification of migration & invasion assays in RM-1 and PC-3 cells. Bars, 100 μm and 50 μm. ns, not significant; one-way ANOVA. (**G**) GSEA analysis identifying negative regulation of immune response and negative regulation of IFN-γ production signatures as the top activated pathways in *BHLHE22*-high patients (top 50% quantile) from the TCGA-PRAD datasets. GSEA analysis identifying negative regulation of immune response and negative regulation of T cell-mediated immunity signatures as the top activated pathways in PC-3-BHLHE22 cells. (**H**) Gene Ontology identifying the immune response gene signature as the top enrichment pathway in PC-3-BHLHE22 cells. (**I**) qRT-PCR analysis of the expression of cell cycle and DNA replication related genes in the indicated cells. ns, not significant; *P < 0.05; one-way ANOVA. (**J**) Cell viability was evaluated by cell cycle using flow cytometry in the indicated cells. Histogram analysis of the cell populations at different phases. ns, not significant; ***P < 0.001; one-way ANOVA. (**K**) Representative images and quantification of colony formation assay in the indicated cells. ns, not significant; ***P < 0.001; one-way ANOVA.

Supplementary Figure 2

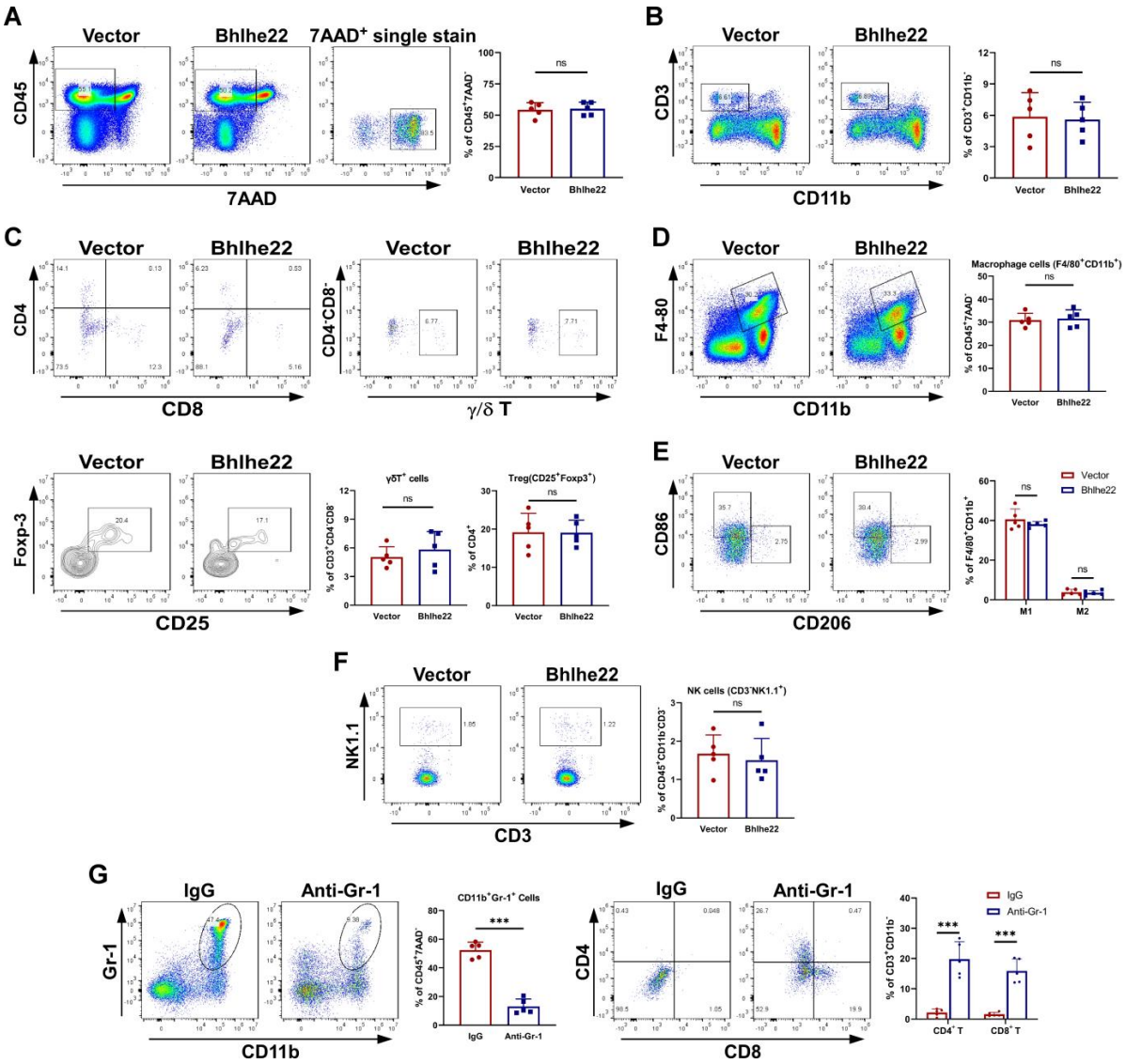

Supplementary Figure 2. BHLHE22 drives an immunosuppressive TME in bone metastasis. (**A** and **B**) Representative plots and quantification of the tumor-infiltrating $CD45^+$ $7AAD^-$ cells (A) and $CD3^+CD11b^-$ (B) cells. ns, not significant; t test. (**C**) Representative plots and quantification of the tumor-infiltrating γ/δ T cells and Tregs. ns, not significant. t test. (**D** to **F**) Representative plots and quantification of the tumor-infiltrating macrophages (D), M1 and M2 macrophages (E), and NK cells (F) in the indicated groups. ns, not significant. t test. (**G**) C57BL/6J mice were LCV-injected with RM-1-Bhlhe22 and randomly divided into anti-Gr-1 and isotype IgGs groups. Representative plots and quantification of the tumor-infiltrating $CD11b^+Gr\text{-}1^+$ cells, $CD4^+$ T and $CD8^+$ T cells in the indicated groups with or without the depletion using anti-Gr-1 antibodies. ***P < 0.001; t test.

Supplementary Figure 3

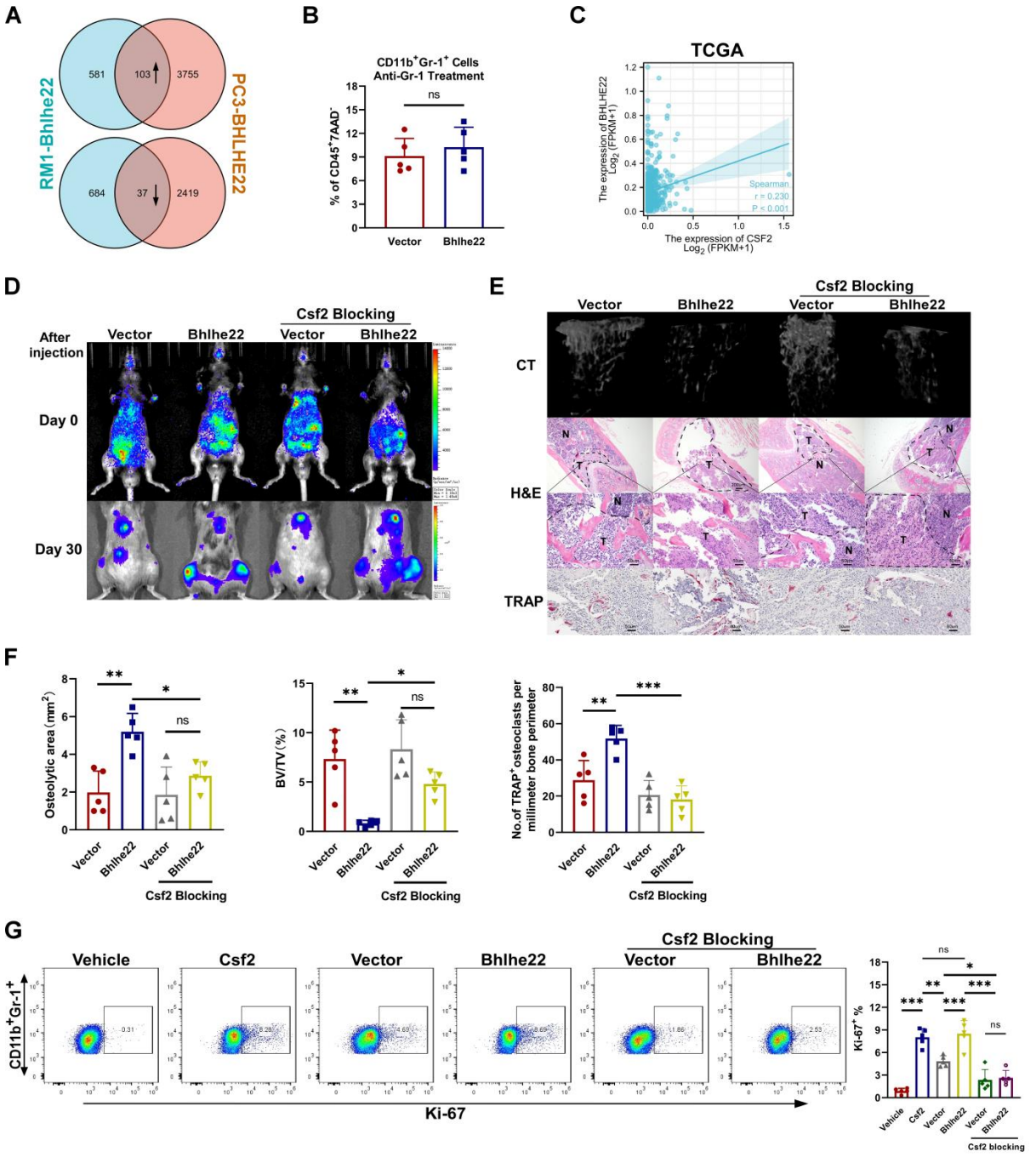

Supplementary Figure 3. BHLHE22 controls immunosuppressive neutrophils and monocytes recruitment and CSF2 serves as a key mediator. (**A**) 103 co-upregulated genes and 37 co-downregulated genes (FC > 1.5) in the RNA-seq datasets. (**B**) Quantification of the $CD11b^{+}Gr\text{-}1^{+}$ cells

infiltration in the indicated groups with the depletion using anti-Gr-1 antibodies. ns, not significant. t test. (**C**) Spearman correlation analysis between *CSF2* and *BHLHE22* expression from the TCGA-PRAD dataset. (**D**) Representative BLI signal of bone metastasis of LCV-injected C57BL/6J mice in the indicated groups. (**E**) Representative micro-CT, H&E (T, tumor; N, the adjacent nontumor tissues. Bars, 200 μm and 50 μm) and TRAP (Bars, 50 μm) images of bone lesions in the indicated groups. (**F**) Quantification of osteolytic areas, bone parameters and $TRAP^{+}$-osteoclasts in the indicated groups. BV/TV, bone/tissue volume ratio. ns, not significant. *P < 0.05, **P < 0.01, ***P < 0.001; one-way ANOVA. (**G**) Representative plots and quantification of the $Ki\text{-}67^{+}CD11b^{+}Gr\text{-}1^{+}$ cells in the indicated groups. ns, not significant. *P < 0.05, **P < 0.01, ***P < 0.001; one-way ANOVA.

Supplementary Figure 4

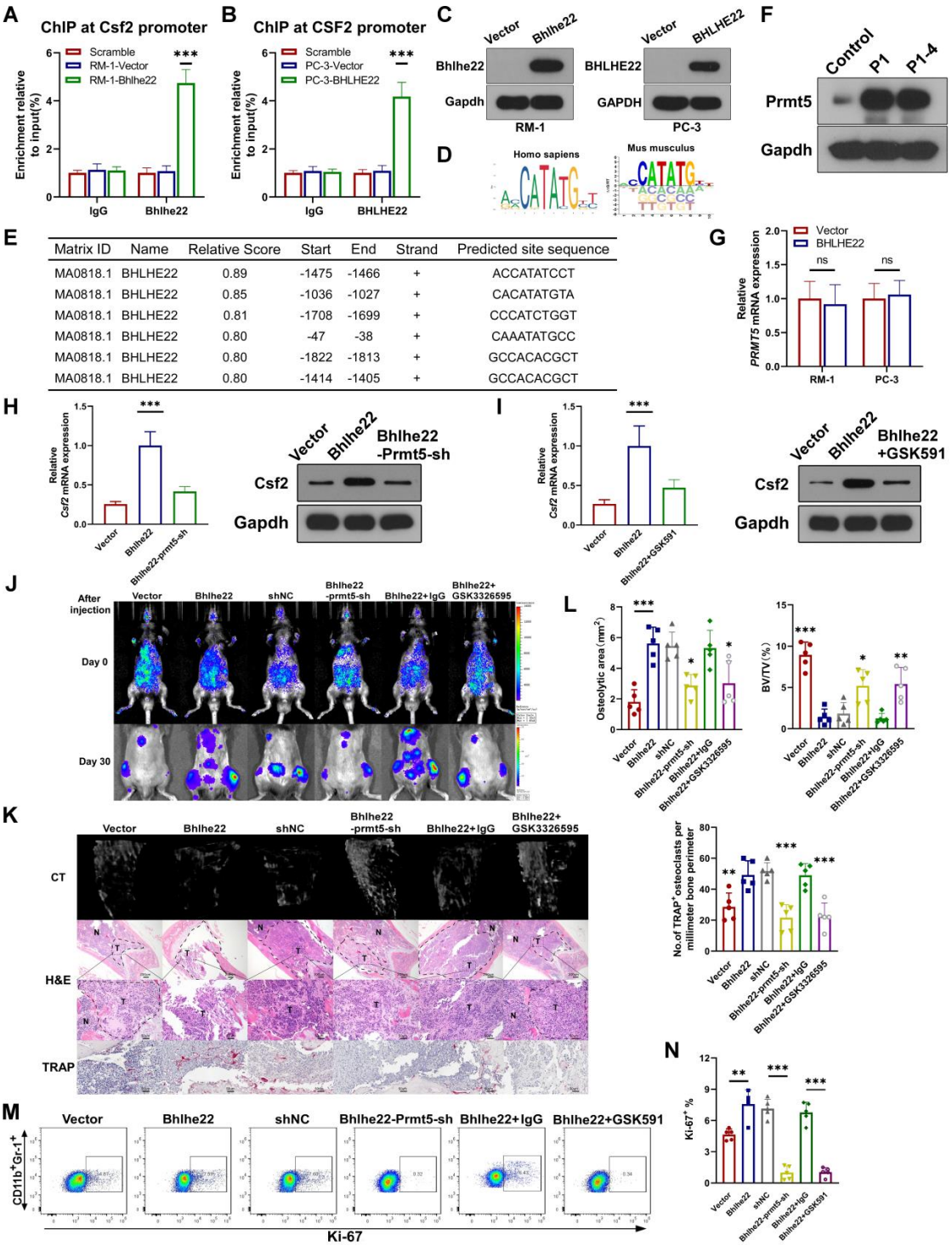

Supplementary Figure 4. BHLHE22 and PRMT5 form a transcriptional complex and transcriptionally activate *CSF2*. (**A**) ChIP-qPCR analysis of Bhlhe22 enrichment on the *Csf2* promoter in RM-1-Vector and RM-1-Bhlhe22 cells. ***P < 0.001; one-way ANOVA. (**B**) ChIP-qPCR analysis of BHLHE22 enrichment on the *CSF2* promoter in PC-3-Vector and PC-3-BHLHE22 cells. ***P < 0.001; one-way ANOVA. (**C**) Western blotting showing BHLHE22 overexpression in RM-1 and PC3 cells. (**D**) The same binding motifs of BHLHE22 in *Homo sapiens* and *Mus musculus* according to the JASPAR and CIS-BP databases. (**E**) Predicted Bhlhe22 binding sites in the mouse *Csf2* promoter. (**F**) Western blotting analysis of the DNA pulldown eluate. (**G**) qRT-PCR analysis of *Prmt5* expression in the indicated cells. ns, not significant; t test. (**H** and **I**) qRT-PCR and western blotting analysis of *Csf2* expression in the indicated cells and groups. ***P < 0.001; one-way ANOVA. (**J**) The effects of Prmt5 inhibited by shRNA and GSK3326595 were evaluated in the LCV-injected mouse model. Bone metastasis was monitored by BLI. (**K**) Representative micro-CT, H&E (T, tumor; N, the adjacent nontumor tissues. Bars, 200 μm and 50 μm) and TRAP (Bars, 50 μm) images of bone lesions in the indicated groups. (**L**) Quantification of osteolytic areas, bone parameters and $TRAP^{+}$-osteoclasts in the indicated groups. BV/TV, bone/tissue volume ratio. *P < 0.05, **P < 0.01, ***P < 0.001; one-way ANOVA. (**M** and **N**) Representative plots and quantification of the $Ki\text{-}67^{+}CD11b^{+}Gr\text{-}1^{+}$ cells in the indicated groups. **P < 0.01, ***P < 0.001; one-way ANOVA.

Supplementary Figure 5

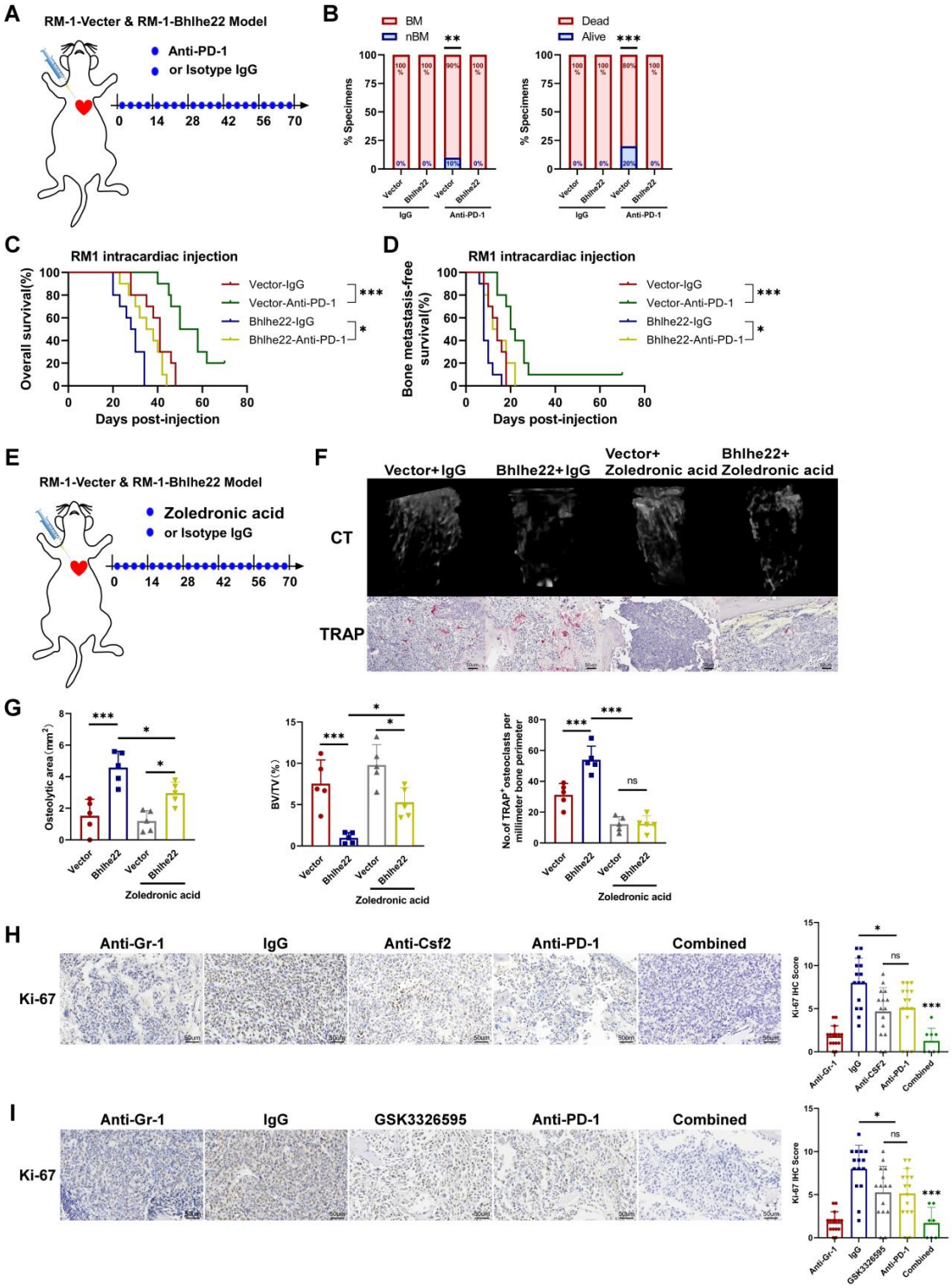

Supplementary Figure 5. CSF2 neutralization/ PRMT5 inhibitor combined with ICT effectively inhibit tumor-infiltrating immunosuppressive neutrophils and monocytes and bone metastasis *in vivo*. (**A**) Investigating the degree of resistance to PD-1 treatment caused by tumoral *Bhlhe22* overexpression. The schedule of treatment in mice LCV-injected with RM-1-Vector and RM-1-Bhlhe22 cells. The mice were treated with IgGs or anti-PD-1 (all n = 10), beginning at day 3 post-injection. (**B**) Incidence of bone metastasis and mortality detected in the indicated groups. **P < 0.01, ***P < 0.001; $\chi 2$ test. (**C** and **D**) Kaplan–Meier analysis of mouse overall (C) and bone metastasis-free (D) survival. *P < 0.05, ***P < 0.001; log-rank test. (**E**) The schedule of osteoclasts inhibition experiment in mice LCV-injected with RM-1-Vector and RM-1-Bhlhe22 cells. The mice were treated with IgGs or zoledronic acid (all n = 5), beginning at day 3 post-injection. (**F**) Representative micro-CT and TRAP (Bars, 50 μm) images of bone lesions in the indicated groups. (**G**) Quantification of osteolytic areas, bone parameters and $TRAP^+$-osteoclasts in the indicated groups. BV/TV, bone/tissue volume ratio. ns, not significant. *P < 0.05, ***P < 0.001; one-way ANOVA. (**H** and **I**) IHC analysis and staining score of Ki-67 in bone metastases of mice LCV-injected with RM-1-Bhlhe22. All treatments are shown in the upper part. Bars, 50 μm. ns, not significant. *P < 0.05, ***P < 0.001; one-way ANOVA.

Supplementary Figure 6

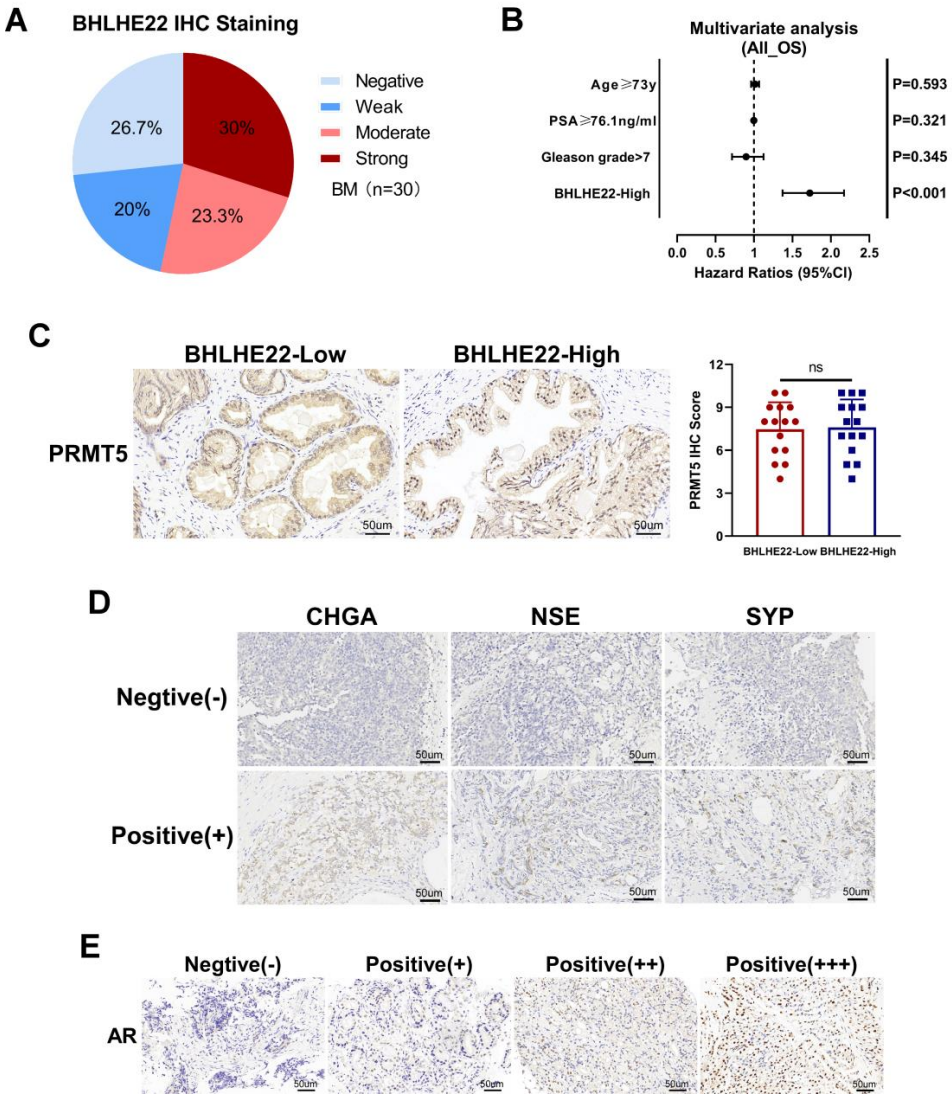

Supplementary Figure 6. Potential role for BHLHE22 as a biomarker for ICT combination therapies in bone metastatic PCa. (**A**) The distribution of BHLHE22 staining in BM samples of patients with PCa (n = 30). (**B**) The significance of the association between the BHLHE22-High signature and OS together with other important clinical variables assessed using multivariate Cox regression analysis. (**C**) IHC analysis and staining score of PRMT5 in BM samples of patients with PCa (n = 30). Patients were stratified by low (bottom 50% quantile) and high (top 50% quantile) BHLHE22 expression. Bars, 50 μm. ns, not significant; t test. (**D** and **E**) Representative IHC staining images of AR and NE status in PCa tissue samples.

References

1. Ren, D.*, et al*. Wnt5a induces and maintains prostate cancer cells dormancy in bone. *J Exp Med*. **216**, 428-449 (2019).
2. Livak, K.J. & Schmittgen, T.D. Analysis of relative gene expression data using real-time quantitative PCR and the 2(-Delta Delta C(T)) Method. *Methods*. **25**, 402-408 (2001).
3. Lang, C.*, et al*. m(6) A modification of lncRNA PCAT6 promotes bone metastasis in prostate cancer through IGF2BP2-mediated IGF1R mRNA stabilization. *Clinical and translational medicine*. **11**, e426 (2021).
4. Croucher, P.I.*, et al*. Zoledronic acid treatment of 5T2MM-bearing mice inhibits the development of myeloma bone disease: evidence for decreased osteolysis, tumor burden and angiogenesis, and increased survival. *J. Bone Miner. Res.* **18**, 482-492 (2003).
5. Zhuang, J.*, et al*. Osteoclasts in multiple myeloma are derived from Gr-1+CD11b+myeloid-derived suppressor cells. *PLoS One*. **7**, e48871 (2012).
6. Gao, J.*, et al*. Integrative analysis of complex cancer genomics and clinical profiles using the cBioPortal. *Sci Signal*. **6**, pl1 (2013).
7. Cerami, E.*, et al*. The cBio cancer genomics portal: an open platform for exploring multidimensional cancer genomics data. *Cancer Discov.* **2**, 401-404 (2012).